RESEARCH ARTICLE

Recent shortening of the mature tropical cyclone stage over the western North Pacific

Jinjie Song[1,2] 🄳 | Philip J. Klotzbach[3] | Sulin Jiang[1,2] | Yihong Duan[2]

[1]Nanjing Joint Institute for Atmospheric Sciences, Chinese Academy of Meteorological Sciences, Nanjing, China

[2]State Key Laboratory of Severe Weather, Chinese Academy of Meteorological Sciences, Beijing, China

[3]Department of Atmospheric Science, Colorado State University, Fort Collins, Colorado, USA

Correspondence
Jinjie Song, Nanjing Joint Institute for Atmospheric Sciences, Chinese Academy of Meteorological Sciences, 8 Yushun Road, Nanjing, 210041, China.
Email: songjinjie@qq.com

Funding information
National Natural Science Foundation of China, Grant/Award Numbers: 41905001, 42175007, 42192552, 42192554, 61827901, U2342203; G. Unger Vetlesen Foundation

Abstract

This study investigates long-term trends related to the mature stage duration of tropical cyclones (TCs) over the western North Pacific (WNP) during June–November between 1982 and 2021. There is a significant shortening in the mean duration of the WNP mature TC stage, which is defined as the period when a TC is within 5 kt of its lifetime maximum intensity. This shortening is induced by a significant (weak) poleward migration in the starting (ending) location of the WNP mature TC stage, which can be further explained by changes in environmental conditions. From 1982 to 2021, there have been significant increases in maximum potential intensity and 700–500-hPa relative humidity over most of the WNP, which has broadly expanded the TC-favorable area poleward. Consequently, WNP TCs can start their mature stages and reach their lifetime maximum intensities at higher latitudes. By contrast, there are only weak changes in 850-hPa relative vorticity and 850–200-hPa vertical wind shear (VWS). Given the dominant role of VWS in modulating the TC weakening rate, the TC-suppressive area over the subtropical WNP has shown lesser changes, thus leading to insignificant changes in the ending location of the mature TC stage.

KEYWORDS
mature stage, tropical cyclone, typhoon, western North Pacific

1 | INTRODUCTION

Tropical cyclones (TCs) are among the most devastating natural disasters around the world, leading to large economic losses as well as casualties for TC-prone coastal and adjacent inland regions. In general, a life cycle of TC can be categorized into genesis, intensification, mature, and weakening/transitioning stages (e.g., Dunn & Miller, 1960; Riehl, 1954; Simpson & Riehl, 1981). The mature stage is often regarded as the quasi-steady state with only slight intensity fluctuations around the time when a TC reaches its lifetime maximum intensity (LMI), while other stages are characterized by more significant changes in TC intensity. TC intensity changes significantly correlate with various environmental factors including sea surface temperature (SST), maximum potential intensity (MPI; Emanuel, 1988), relative humidity at various levels, low-level relative vorticity, upper-level divergence, and vertical wind shear (VWS) (e.g., DeMaria & Kaplan, 1994, 1999; Knaff et al., 2005).

Recent studies have reported increasing trends in both TC intensification and weakening rates since the

1980s, associated with increasing occurrence proportions of both rapid intensification and rapid weakening (Bhatia et al., 2019; Bhatia et al., 2022; Kishtawal et al., 2012; Song et al., 2020). Kishtawal et al. (2012) also noted a significant decreasing trend in the average timespan for strong TCs (e.g., LMI $\geq$80 kt) intensifying from 64 kt to their LMIs during 1986–2010. Furthermore, Wang et al. (2020) showed a significant reduction in the average lifetime of TCs that reached major hurricane/typhoon intensity (Saffir-Simpson Hurricane Wind Scale Category 3 or higher; one-minute maximum sustained wind $\geq$96 kt) from 1982 to 2018. They linked this reduction to an increase in the average TC LMI. Given that TCs with larger LMIs exhibited more rapid intensification and weakening rates, they spent less time intensifying from Category 1 to 3 and weakening from Category 3 to 1. This also implied that the early intensification (Category 1–3) and final weakening (Category 3–1) stages of major TCs occurred more quickly. Both Kishtawal et al. (2012) and Wang et al. (2020) focused on duration changes related to the strongest TCs.

By comparison, less attention has been paid to changes in the mature TC stage duration. Wang et al. (2020) found an insignificant trend in the time when a TC was at major TC intensity. This analysis, however, may consider the final intensification, mature, and early weakening stages together. Kossin et al. (2014) noted a significant poleward migration of the average location of TC LMI during recent decades. This implies a more favorable mid-latitude environment for TC development. Also given that TCs often decay when moving into the mid-latitudes, the change in time that a TC can maintain its LMI remains uncertain.

In this study, we are not just concerned with major hurricanes/typhoons. We specifically focus on when TCs are near their LMIs. Hence, the objective of this study is to investigate trends related to the duration of the mature TC stage. We focus on the western North Pacific (WNP), which is the climatologically most TC-active basin worldwide, with approximately one-third of global TCs on an annually averaged basis (Lee et al., 2012).

2 | DATA AND METHODOLOGY

WNP TC best track data are obtained from the Joint Typhoon Warning Center (JTWC), including 6-h TC center position and 1-min maximum sustained wind (V_{MAX}), as compiled in the International Best Track Archive for Climate Stewardship (IBTrACS) v04r00 (Knapp et al., 2010). We focus on the period of 1982–2021, because of the relatively low reliability of TC intensity estimates due to lack of global satellite coverage prior to

the early 1980s (Kossin et al., 2014). We analyze the season spanning June–November (JJASON), given that approximately 85% of the annual total number of WNP TCs formed during this period (Song & Klotzbach, 2019). To reduce the uncertainty in detecting weak TCs and short-lived TCs (Klotzbach & Landsea, 2015), we only consider TCs reaching an LMI of at least 64 kt (e.g., typhoons) and maintaining 34-kt intensity for at least 48 h. Our results are not significantly changed if all TCs reaching an LMI of at least 34 kt are considered or TC records at longer time intervals (e.g., 12 or 24 h) are used (figures not shown).

There have been notable changes in how TC intensity has been measured by JTWC since the start of our study period in 1982. As JTWC began phasing out aircraft reconnaissance, the percentage of TC intensity estimations based on aircraft reconnaissance dropped from ~35% in 1982 to ~10% in 1986 (Guard et al., 1992). When JTWC terminated its aircraft reconnaissance missions in 1987, satellites became the dominant platform for TC warnings over the WNP (Guard et al., 1992). However, given the relatively short life span of satellites and regular upgrades in satellite-related techniques, multiple satellites have been used for observing TCs during our study period (Kossin et al., 2013). To gauge the impact of this inhomogeneity on TC-observing techniques, we also analyzed TC data from the Advanced Dvorak Technique-Hurricane Satellite-B1 data (ADT-HURSAT; Kossin et al., 2020) during 1982–2017. The ADT-HURSAT data are more homogeneous and have been widely used to analyze trends related to TC intensity (e.g., Kossin et al., 2013; Kossin et al., 2020).

The mature stage is defined as the period when the TC intensity is in a quasi-steady state with only small fluctuations around the LMI (Dunn & Miller, 1960; Riehl, 1954; Simpson & Riehl, 1981). We applied a threshold V_0 to measure whether the intensity fluctuation was significant. We initially identified the time that a TC first attained its LMI (t_{LMI}) and then traced the remaining records for that TC forward and backward from t_{LMI} until the criterion $|V_{MAX} - LMI| \leq V_0$ was not satisfied. The total period around the t_{LMI} was regarded as the mature TC stage. In this study, we used a 5 kt threshold for V_0, which is the minimum interval for TC intensity records in the JTWC best track data. Our results are not significantly changed if other thresholds (e.g., 0, 10 kt) are used (Figure 1a). The 6-h records during the mature TC stage are summed over a $5° \times 5°$ grid to represent the occurrence number. The occurrence number is then divided by the total occurrence number over the WNP to obtain the occurrence percentage. The mature stage can also be identified using a percentage-based threshold, applying the criterion $V_{MAX} \geq p\% \times LMI$. Our results show little
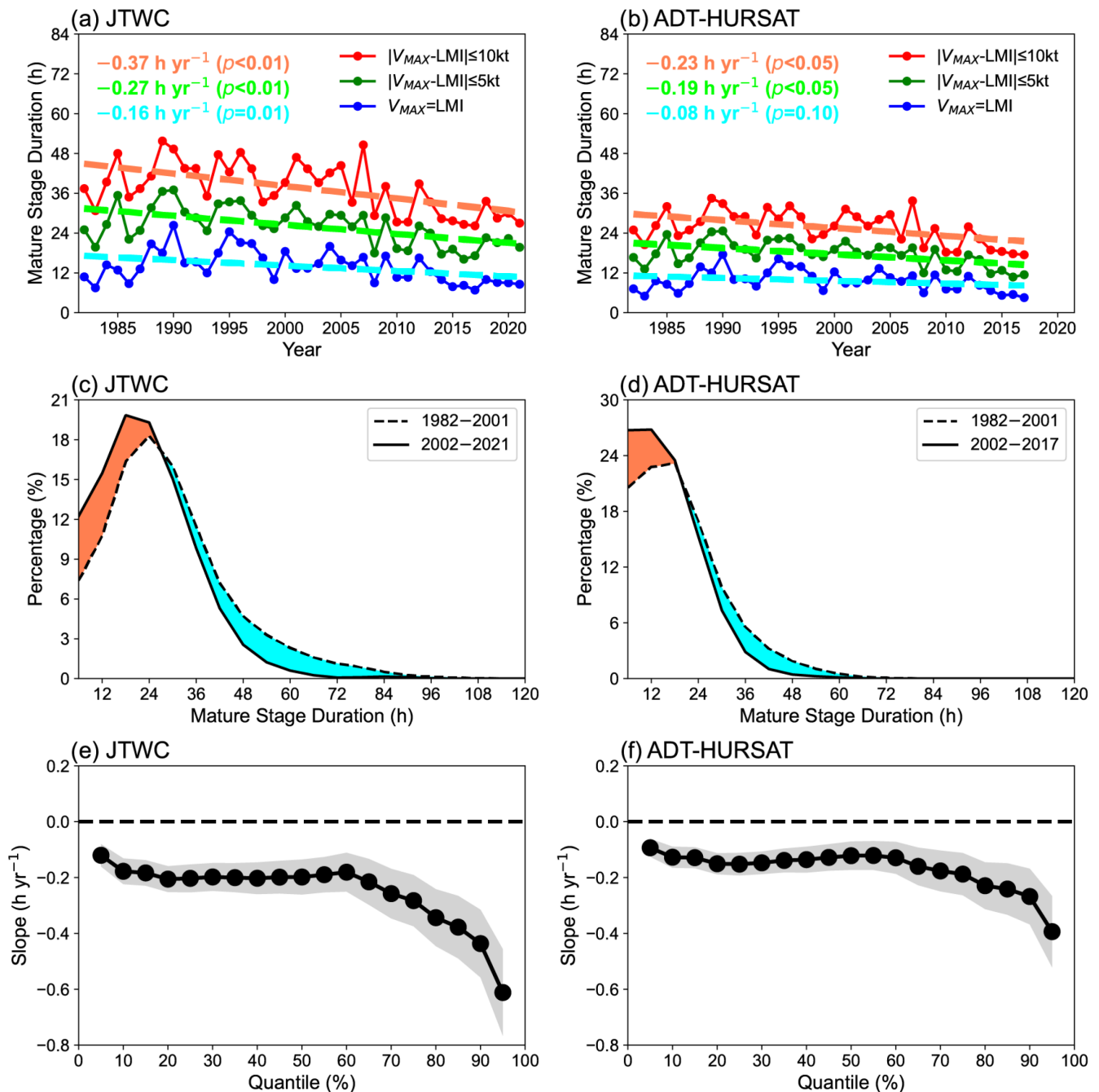
FIGURE 1 (a), (b) Annual mean duration of the WNP mature TC stage for the (a) JTWC and (b) ADT-HURSAT datasets. Linear trends obtained through least-squares are shown by dashed lines, while their slopes and significance levels based on a Student's *t*-test are also displayed in the panel. (c), (d) Difference in the distributions of mature stage durations for WNP TCs obtained from the (c) JTWC and (d) ADT-HURSAT datasets between the two sub-periods. (e), (f) Slope of the quantiles for WNP TC mature stage durations obtained from (e) the 1982–2021 JTWC dataset and (f) the 1982–2017 ADT-HURSAT dataset. Circles represent the slope derived by the least-squares of the mature stage duration as a function of year for each quantile from 5% to 95% in 5% intervals. Filled circles indicate slopes that are significant at the 0.05 level according to a Student's *t*-test. Shading denotes the standard error of the estimated slope, representing the average distance that the original values fall from the regression line.

change when a *p*-value of 80, 90, or 95 is used (figure not shown).

Monthly mean SST data over a $1° \times 1°$ grid are obtained from the Hadley Centre Sea Ice and Sea Surface

Temperature dataset (HadISST; Rayner et al., 2003). Monthly atmospheric fields are derived from the fifth-generation European Centre for Medium-Range Weather Forecasts reanalysis of the global climate (ERA5;

Hersbach et al., 2020) with a resolution of $0.25° \times 0.25°$. Four large-scale environmental variables influencing TC intensity change are considered here: MPI, 700–500-hPa relative humidity, 850-hPa relative vorticity, and 850–200-hPa VWS.

Statistical significance is determined by a two-tailed Student's t-test.

3 | RESULTS

3.1 | Trends related to mature stage duration

Figure 1a displays a significant decreasing trend in the mean duration of the WNP mature TC stage between 1982 and 2021, regardless of whether a 0-kt, 5-kt, or 10-kt mature intensity change threshold is used. As this threshold increases, the duration of the mature stage increases and its decreasing rate since 1982 also strengthens. When considering the 5-kt threshold, the mature stage duration decreases at a rate of 0.27 h years^{-1} ($p < 0.01$), equivalent to a 24% reduction from 1982 to 2021. By comparison, the decreasing trends in the mean TC mature stage duration for ADT-HURSAT are smaller than those for JTWC (Figure 1b). We do find significant decreasing trends at the 0.05 level if a 5-kt or 10-kt threshold is used, while the trend significance is at the 0.10 level when using a 0-kt threshold.

Moreover, the distribution of the mature stage duration for WNP TCs exhibits an overall shift toward smaller values during 1982–2021 (Figure 1c). There are increases (decreases) in the percentages of TCs with a mature stage duration of $\leq$24 h (>24 h) from 1982–2001 to 2002–2021. The mean mature stage duration has been reduced from 29 h for 1982–2001 to 23 h for 2002–2021. Similarly, the distribution of the mature stage duration for ADT-HURSAT shifts toward smaller values during 1982–2017 (Figure 1d). Consistent with this distribution change, all quantiles for the mature stage duration for WNP TCs show significant decreasing trends from 1982 to 2021 (Figure 1e). The slopes are approximately −0.20 h years^{-1} for quantiles lower than 60% and become more negative as the quantiles increase. In particular, the most negative slope is shown for the 95th quantile, implying that the duration of the longest-lived mature TCs decreases more significantly than that of shorter-lived mature TCs (Figure 1e). A similar pattern is also observed in the trends of the duration quantiles for ADT-HURSAT, although at smaller magnitudes (Figure 1f).

Figure 2a displays a significant inverse relationship between mature stage duration and the LMI ($r = -0.22$;

$p < 0.01$). We find that TCs with larger LMIs tend to exhibit shorter mature stage durations, consistent with Wang et al. (2020). During 1982–2021, there is a significant increasing trend in the annual mean LMI over the WNP (Figure 2b), as noted in previous publications (e.g., Kossin et al., 2013). To minimize the influence of LMI on the mature stage duration, we apply a linear relationship (the dashed line as shown in Figure 2a) to obtain duration anomalies. Figure 2c displays a significant decrease in the mature stage duration anomaly, with a slope of −0.25 h years^{-1} ($p < 0.01$). This decrease is just slightly smaller than our original result calculated with LMI included (−0.27 h years^{-1}). This result means that the decreasing trend in mature stage duration is less influenced by the increasing LMI trend, as would be expected given the small variance in the duration explained by LMI (~5%).

Furthermore, the mature stage duration is defined to be the distance traveled divided by the translation speed during the mature stage. Figure 2d shows a significant relationship between the duration and the distance traveled during the mature stage ($r = 0.76$; $p < 0.01$). This indicates that TCs with a longer mature duration often travel farther during their mature stage. Consistent with the decreasing mature stage duration, there is a significant decreasing trend in the annual mean distance traveled during the mature stage from 1982 to 2021, with a decreasing trend of −4.2 km years^{-1} ($p < 0.01$) (Figure 2e). The change in the distance traveled is well correlated with the latitudinal distance traveled ($r = 0.87$; $p < 0.01$). The latitudinal distance traveled during the mature stage has decreased at a rate of −0.026° years^{-1} ($p = 0.01$), indicating that TC maturity tends to occur within a narrower latitudinal belt. This decrease in latitudinal distance can be explained by the start of the mature stage shifting more poleward than the end of the mature stage (Figure 2f). The starting location of the mature stage has significantly migrated northward at a rate of 0.047° years^{-1} ($p = 0.02$), far exceeding the northward migration rate of the ending location (0.021° years^{-1}; $p = 0.42$).

The other contributor, average translation speed, during the mature stage shows only a weak correlation with the duration ($r = -0.06$; $p = 0.13$) (Figure 2g). We find an insignificant trend in the annual mean translation speed during the mature stage (Figure 2h). These results mean that significant decreases in the latitudinal distance traveled during the mature stage are predominately associated with the shortening of the mature stage duration, while changes in translation speed play a lesser role.

Figure 3a displays spatial trends in WNP TC genesis percentage. More TCs form over a region spanning 120°–150° E, while fewer TCs form outside of this region.
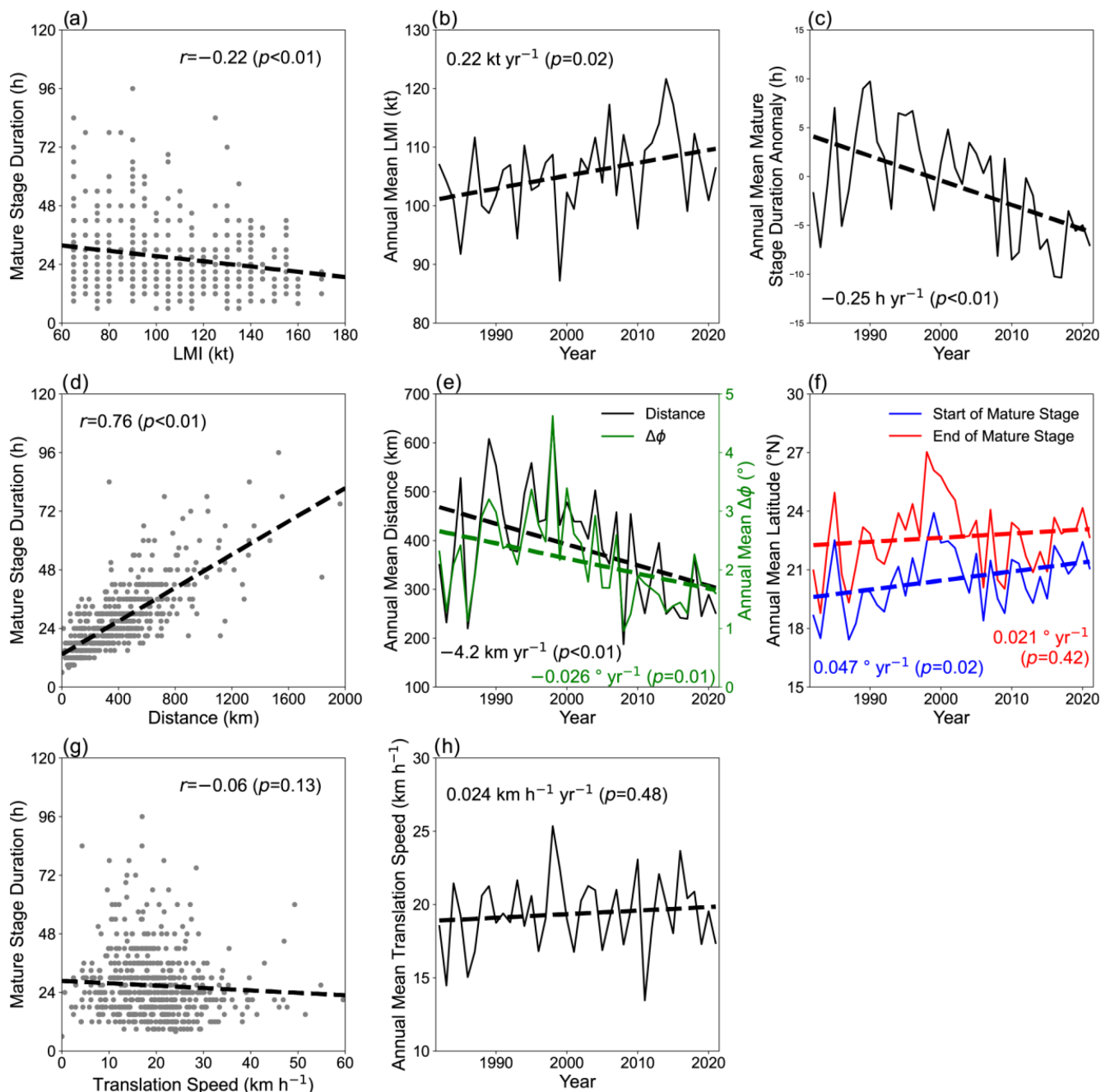
FIGURE 2   (a), (d), (g) Relationships of duration versus (a) LMI, (d) distance traveled and (g) average translation speed during the mature TC stage over the WNP. Dashed lines are obtained by using least-squares. Correlations and the corresponding significance levels based on a Student's t-test are given in the panel. (b), (c), (e), (f), (h) Annual mean (b) LMI, (c) mature stage duration anomaly obtained by linearly removing the effect of LMI, (e) distance traveled and latitude during the mature stage, (f) starting and ending latitudes of the mature stage and (h) average translation speed during the mature stage from 1982 to 2021. Linear trends obtained through least-squares are shown by dashed lines, while their slopes and significance levels based on a Student's t-test are also displayed for each panel.

However, there are no significant changes in TC genesis percentage over the entire WNP. By contrast, the long-term changes in TC occurrence percentage during the mature stage exhibit a north–south dipolar structure (Figure 3b). Large changes occur over the region bounded by 10°–25° N, 105°–155° E, where mature TC stages occur the most frequently, with significant decreases south of 20° N and significant increases north of 20° N. This pattern is consistent with a significant northward shift of the starting location of the mature stage.

During 1982–2021, there is only a weak poleward migration in the annual mean TC genesis latitude (Figure 3c). There is also an insignificant relationship
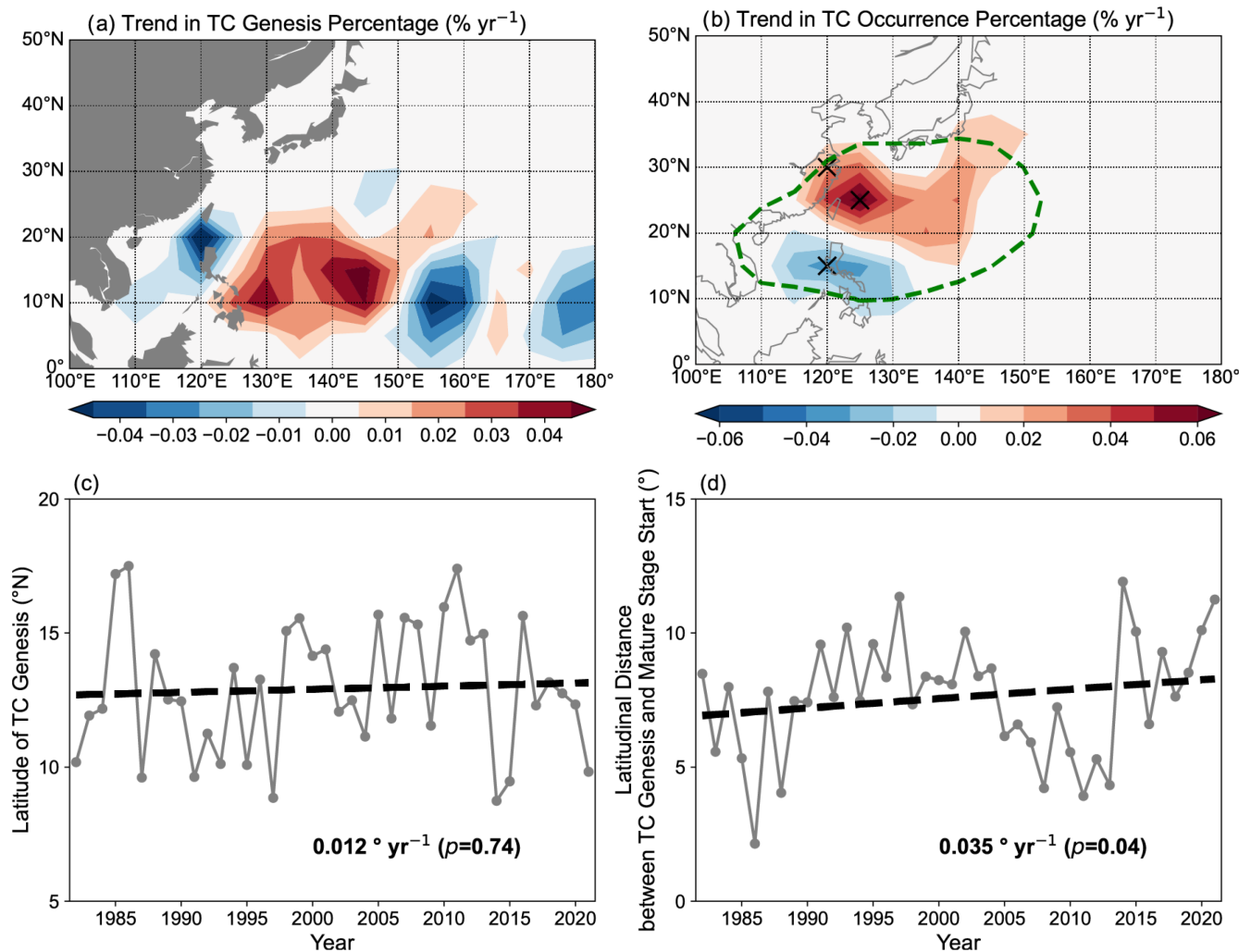
FIGURE 3 (a), (b) Trends in (a) TC genesis percentage and (b) TC occurrence percentage during the mature stage from 1982 to 2021. Black crosses refer to trends that are significant at the 0.05 level based on a Student's *t*-test. The area bounded by the green dashed line in (b) denotes the main region with 95% of the total occurrences of mature TCs. (c), (d) Annual mean (c) TC genesis latitude and (d) latitudinal distance between TC genesis location and starting position of the TC mature stage from 1982 to 2021. Linear trends obtained through least-squares are shown by dashed lines, while their slopes and significance levels based on a Student's *t*-test are also displayed for each panel.

between the mature stage duration and the genesis latitude ($r = 0.15$; $p = 0.37$), implying that the TC mature stage duration is less influenced by shifts in TC genesis location. Figure 3d shows a significant increasing trend in the distance between TC genesis latitude and the starting latitude of the TC mature stage, accounting for ~74% of the trend in the mature stage starting latitude. These results mean that changes in TC genesis latitude only have a minor impact on the northward shift of the TC mature stage.

3.2 | Trends in environmental conditions

These changes related to the mature TC stage can be explained by trends in large-scale environmental conditions

over the WNP from 1982 to 2021 (Figure 4). The patterns displayed in Figure 4 are in broad agreement with the environmental changes between 1990 and 2021 reported by Klotzbach et al. (2022). There are significant increases in SST and MPI over most of the WNP (Figure 4a, c), as noted in Klotzbach et al. (2022). Given that the magnitude of SST increases is much greater in the extratropics than in the tropics, large changes in the SST gradient mainly occur between 30° and 50° N (Figure 4b). Over the main region with the highest occurrence of mature TCs, there are only weak changes in the SST gradient. Significant decreases in 700–500-hPa relative humidity occur over the East Asian continent, while significant humidity increases are concentrated over a belt from the equatorial western Pacific to the subtropical central Pacific (Figure 4d).

By comparison, there are only weak trends in dynamic variables (e.g., 850-hPa relative vorticity and
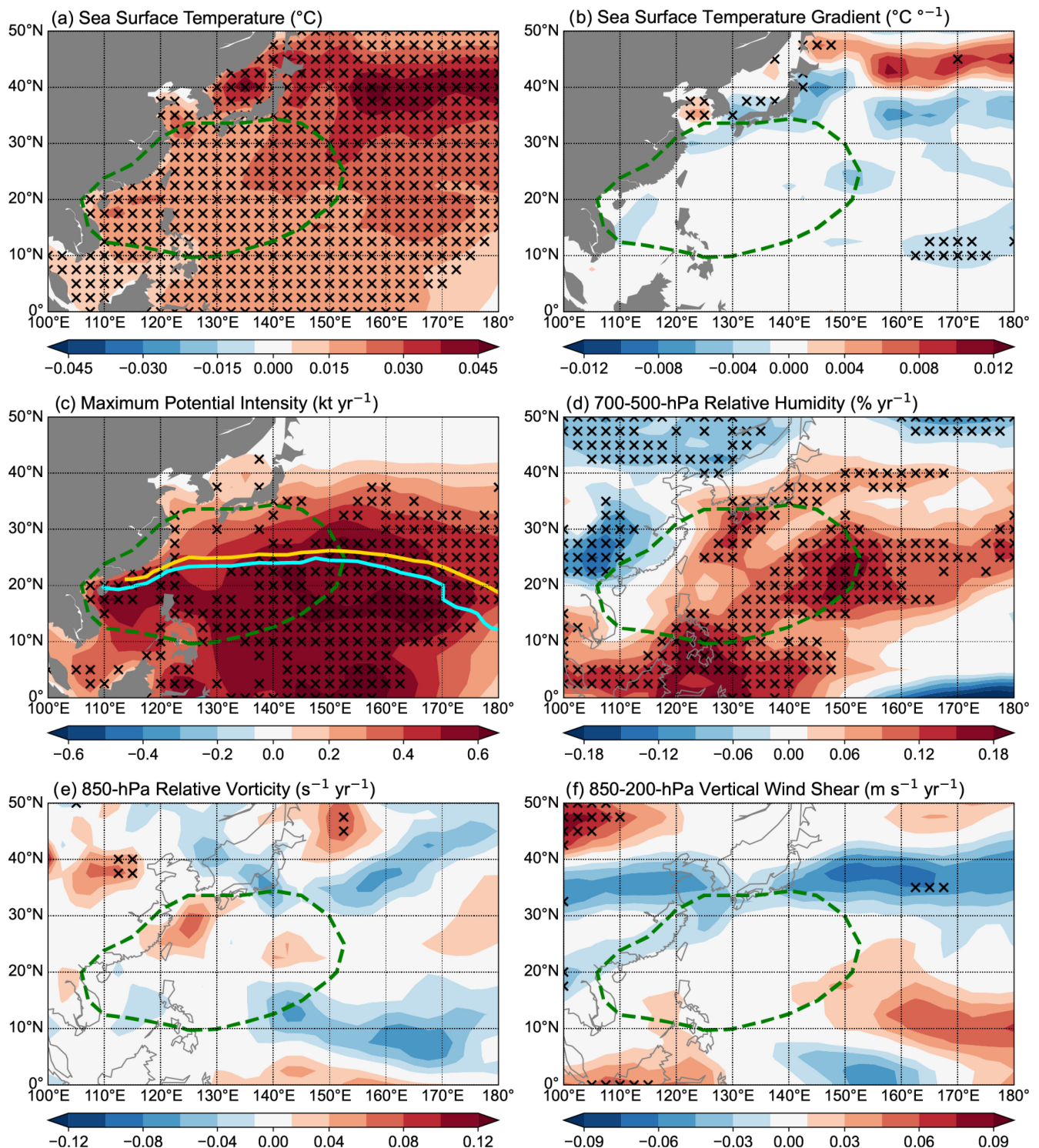
FIGURE 4 Trends in (a) SST, (b) SST gradient, (c) MPI, (d) 700–500-hPa relative humidity, (e) 850-hPa relative vorticity and (f) 850–200-hPa vertical wind shear from 1982 to 2021. The area bounded by the green dashed line denotes the region with 95% of the total occurrences of mature TCs. Black crosses refer to trends significant at the 0.05 level based on a Student's *t*-test. In (c), blue and yellow lines denote the 960 hPa MPI contours in 1982–2001 and 2002–2021, respectively.

850–200-hPa VWS) over the WNP from 1982 to 2021 (Figure 4e, f). These results imply that changes in dynamic variables play a lesser role in modulating the long-term trend in WNP TC intensification. Decreases in VWS occur within a latitudinal belt spanning 30°–40° N, corresponding to the northern boundary of the main region with high mature TC occurrences (Figure 4f).

Hart and Evans ([2001](#)) defined the 960-hPa MPI contour as the northern boundary at which tropical development was no longer possible. TCs tended to intensify (decay) south (north) of the 960-hPa MPI contour. From 1982–2001 to 2002–2021, the 960-hPa MPI contour shifted northward (Figure [4c](#)), consistent with the basin-wide increase in MPI. South of the 960-hPa MPI contour, the MPI and other thermodynamic variables (e.g., SST and relative humidity) have become more favorable for TC development. Meanwhile, the region with tropical development has expanded poleward, meaning that WNP TCs can undergo intensification over a larger region. Accordingly, WNP TCs have started their mature stage and reached their LMIs at higher latitudes.

By comparison, north of the 960-hPa MPI contour, TCs generally decay due to lack of tropical development, although there are significant increases in SST, MPI, and relative humidity. Ma et al. ([2019](#)) and Fei et al. ([2020](#)) both reported that these thermodynamic factors played a lesser role in controlling the TC decay rate. Instead, the SST gradient and VWS have been shown to be the primary drivers of the WNP TC decay rate, contributing 18.3% and 14.9% to the TC weakening rate, respectively (Fei et al., [2020](#); Ma et al., [2019](#)). Since there are only weak decreases in both the SST gradient and VWS in the region favorable for TC weakening over the subtropical WNP (Figure [4b, f](#)), the ending location of the mature TC stage has exhibited an insignificant poleward migration.

4 | SUMMARY

This study investigates trends related to the duration of the WNP mature TC stage during JJASON between 1982 and 2021, as well as their environmental contributors. The mature TC stage is defined as the period when the TC intensity is in a quasi-steady state, with its difference relative to the LMI being ≤ 5 kt. There is a significant shortening in the mean duration of the WNP mature TC stage, with a rate of -0.27 h years^{-1} ($p < 0.01$). We primarily link this significant reduction to the mean distance traveled by mature TCs, while only finding a weak relationship with changes in the mean translation speed. We further note a significant (weak) poleward migration in the starting (ending) location of the WNP mature TC stage.

These changes in the starting and ending locations of the mature stage can be explained by trends in different environmental variables. During the period of 1982–2021, there are significant increases in MPI and 700–500-hPa relative humidity over most of the WNP, while only weak changes in 850-hPa relative vorticity and 850–200-hPa VWS occur.

On one hand, more favorable thermodynamic conditions have enlarged the region with TC-favorable conditions. As a result, WNP TCs can start their mature stages and subsequently reach their LMIs at higher latitudes. On the other hand, over the subtropical WNP, the TC weakening rate is significantly modulated by the SST gradient and VWS. These two variables have not changed much in the subtropics from 1982 to 2021, leading to insignificant changes in the ending latitude of the mature TC stage.

Our results imply that although the average LMI of WNP TCs has increased during recent decades, TCs tend to maintain their LMIs for a shorter period and begin to decay sooner. This shortening of the mature stage tends to be jointly induced by significantly enhanced TC-favorable conditions in the tropics and nearly unchanged TC-suppressing conditions in the subtropics. Additionally, Kossin et al. ([2013](#)) reported a larger increase in LMIs of TCs with greater intensities. We intend to investigate whether the mature stage duration of stronger TCs shortens at a greater rate. Our results are also helpful for improving intensity prediction during the mature TC stage. Future work will further investigate changes in the mature TC stage duration and the associated physical mechanisms through numerical model experiments.

AUTHOR CONTRIBUTIONS
Jinjie Song: Conceptualization; formal analysis; investigation; methodology; supervision; writing – original draft; writing – review and editing. **Philip J. Klotzbach:** Investigation; writing – review and editing. **Sulin Jiang:** Formal analysis; methodology. **Yihong Duan:** Resources; supervision.

DATA AVAILABILITY STATEMENT
All data used in this study are freely available online. Western North Pacific TC best track data provided in IBTrACS are available at: https://doi.org/10.25921/82ty-9e16. ADT-HURSAT data are downloaded at: https://www.pnas.org/doi/10.1073/pnas.1920849117#supplementary-materials. Monthly mean SST data provided by the Hadley

Centre Sea Ice and Sea Surface Temperature (HadISST) are obtained from: https://www.metoffice.gov.uk/hadobs/hadisst/data/download.html. The fifth generation European Centre for Medium–Range Weather Forecasts atmospheric reanalysis of the global climate (ERA5) is retrieved from: https://doi.org/10.24381/cds.143582cf.

ORCID

Jinjie Song https://orcid.org/0000-0003-3948-8894

REFERENCES

Bhatia, K., Baker, A., Yang, W., Vecchi, G., Knutson, T., Murakami, H. et al. (2022) A potential explanation for the global increase in tropical cyclone rapid intensification. *Nature Communications*, 13, 6626.

Bhatia, K., Vecchi, G.A., Knutson, T.R., Murakami, H., Kossin, J., Dixon, K.W. et al. (2019) Recent increases in tropical cyclone intensification rates. *Nature Communications*, 10, 635.

DeMaria, M. & Kaplan, J. (1994) A statistical hurricane intensity prediction scheme (SHIPS) for the Atlantic basin. *Weather and Forecasting*, 9, 209–220.

DeMaria, M. & Kaplan, J. (1999) An updated statistical hurricane intensity prediction scheme (SHIPS) for the Atlantic and eastern North Pacific basins. *Weather and Forecasting*, 14, 326–337.

Dunn, G.E. & Miller, B.I. (1960) *Atlantic hurricanes*. Baton Rouge, LA: Louisiana State University Press, p. 326.

Emanuel, K.A. (1988) The maximum intensity of hurricanes. *Journal of Atmospheric Sciences*, 45, 1143–1155.

Fei, R., Xu, J., Wang, Y. & Yang, C. (2020) Factors affecting the weakening rate of tropical cyclones over the western North Pacific. *Monthly Weather Review*, 148, 3693–3712.

Guard, C.P., Carr, L.E., Wells, F.H., Jeffries, R.A., Gural, N.D. & Edson, D.K. (1992) Joint typhoon warning center and the challenges of multibasin tropical cyclone forecasting. *Weather and Forecasting*, 7, 328–352.

Hart, R.E. & Evans, J.L. (2001) A climatology of extratropical transition of Atlantic tropical cyclones. *Journal of Climate*, 14, 546–564.

Hersbach, H., Bell, B., Berrisford, P., Hirahara, S., Horányi, A., Muñoz-Sabater, J., Nicolas, J., Peubey, C., Radu, R., Schepers, D. & Simmons, A. (2020). The ERA5 global reanalysis. *Quarterly Journal of the Royal Meteorological Society*, 146(730), 1999–2049.

Kishtawal, C.M., Jaiswal, N., Singh, R. & Niyogi, D. (2012) Tropical cyclone intensification trends during satellite era (1986-2010). *Geophysical Research Letters*, 39, L10810.

Klotzbach, P.J. & Landsea, C.W. (2015) Extremely intense hurricanes: revisiting Webster et al. (2005) after 10 years. *Journal of Climate*, 28, 7621–7629.

Klotzbach, P.J., Wood, K.M., Schreck, C.J., III, Bowen, S.G., Patricola, C.M. & Bell, M.M. (2022) Trends in global tropical cyclone activity: 1990–2021. *Geophysical Research Letters*, 49, e2021GL095774.

Knaff, J.A., Sampson, C.R. & DeMaria, M. (2005) An operational statistical typhoon intensity prediction scheme for the western North Pacific. *Weather and Forecasting*, 20, 688–699.

Knapp, K.R., Kruk, M.C., Levinson, D.H., Diamond, H.J. & Neumann, C.J. (2010) The international best track archive for climate stewardship (IBTrACS). *Bulletin of the American Meteorological Society*, 91, 363–376.

Kossin, J.P., Emanuel, K.A. & Vecchi, G.A. (2014) The poleward migration of the location of tropical cyclone maximum intensity. *Nature*, 509, 349–352.

Kossin, J.P., Knapp, K.R., Olander, T.L. & Velden, C.S. (2020) Global increase in major tropical cyclone exceedance probability over the past four decades. *Proceedings of the National Academy of Sciences*, 117, 11975–11980.

Kossin, J.P., Olander, T.L. & Knapp, K.R. (2013) Trend analysis with a new global record of tropical cyclone intensity. *Journal of Climate*, 26, 9960–9976.

Lee, T.–.C., Knutson, T.R., Kamahori, H. & Ying, M. (2012) Impacts of climate change on tropical cyclones in the western North Pacific basin. Part I: past observations. *Tropical Cyclone Research and Review*, 1, 213–230.

Ma, Z., Fei, J. & Huang, X. (2019) A definition of rapid weakening for tropical cyclones over the western North Pacific. *Geophysical Research Letters*, 46, 11471–11478.

Rayner, N.A., Parker, D.E., Horton, E.B., Folland, C.K., Alexander, L.V., Rowell, D.P., Kent, E.C. & Kaplan, A. (2003). Global analyses of sea surface temperature, sea ice, and night marine air temperature since the late nineteenth century. *Journal of Geophysical Research: Atmospheres*, 108(D14), 4407.

Riehl, H. (1954) *Tropical meteorology*. New York: McGraw-Hill, p. 392.

Simpson, R.H. & Riehl, H. (1981) *The hurricane and its impact*. Baton Rouge, LA: Louisiana State University Press & Basil Blackwell, p. 398.

Song, J. & Klotzbach, P.J. (2019) Relationship between the Pacific-North American pattern and the frequency of tropical cyclones over the western North Pacific. *Geophysical Research Letters*, 46, 6118–6127.

Song, J., Klotzbach, P.J., Duan, Y. & Guo, H. (2020) Recent increase in tropical cyclone weakening rates over the western North Pacific. *Geophysical Research Letters*, 47, e2020GL090337.

Wang, S., Rashid, T., Throp, H. & Toumi, R. (2020) A shortening of the life cycle of major tropical cyclones. *Geophysical Research Letters*, 47, e2020GL088589.